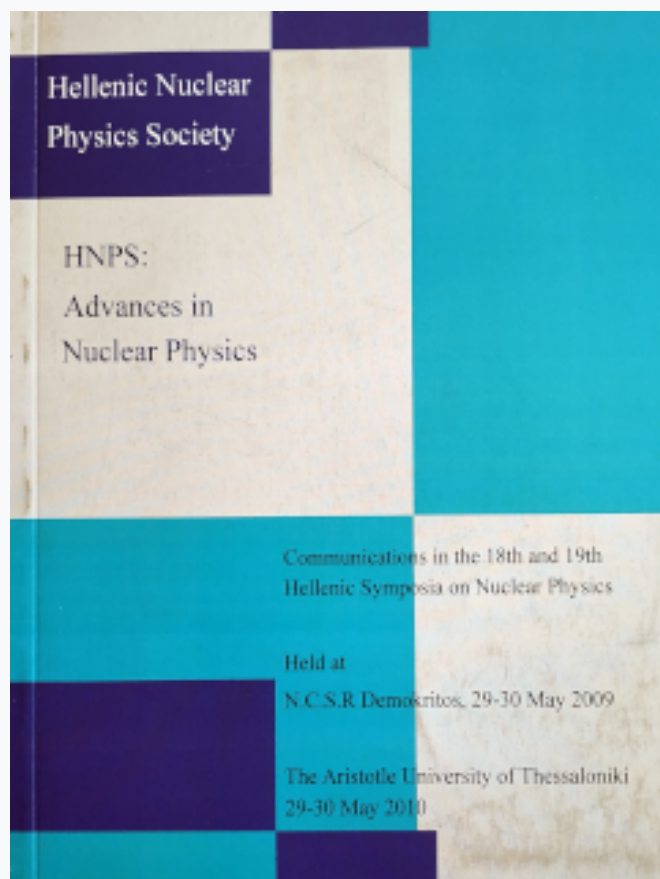


HNPS Advances in Nuclear Physics

Vol 18 (2010)

HNPS2010



To cite this article:

Noli, F., Misaelides, P., Lagoyannis, A., & Riviere, J.-P. (2019). Application of RBS and NRA for the Investigation of Corrosion Resistance of Nitrogen-Implanted Steel. *HNPS Advances in Nuclear Physics*, 18, 113–120.
<https://doi.org/10.12681/hnps.2557>

Application of RBS and NRA for the Investigation of Corrosion Resistance of Nitrogen-Implanted Steel.

F. Noli^{1*}, P. Misaelides¹, A Lagoyannis², J.-P. Rivière³

¹ Department of Chemistry, Aristotle University, GR-54124 Thessaloniki, Greece

² Tandem Accelerator Laboratory, Nuclear Physics Institute, NCSR Demokritos, GR-15310 Aghia Paraskevi- Attiki, Greece

³ Université de Poitiers, Laboratoire de Physique des Matériaux UMR6630-CNRS, 86960 Chasseneuil, Futuroscope Cedex, France

Abstract

Austenitic stainless steel AISI 304L was implanted with low energy, high current nitrogen ions at moderate temperatures extracted from a Kaufman type ion source (Extraction voltage: 1.2 keV; Extracted current: 1 mA/cm²; Ion dose: about 4×10^{19} ions /cm²). The temperature during the implantation (duration 1 hour) was 400 and 500 °C respectively for the two series of samples prepared. The characterization of the samples by X-Ray Diffraction, Transmission Electron Microscopy and Scanning Electron Microscopy showed that a metastable fcc solid solution with a high nitrogen content (about wt. 30%) was formed resulting in an increase of its Vickers hardness. Rutherford Backscattering Spectrometry (E_d : 1.75 MeV) was applied in combination with Nuclear Reaction Analysis (NRA) in order to obtain information about the N-, O- and C- depth distribution in the near-surface layers of the samples. The nitrogen depth distribution was determined using the $^{14}\text{N}(\text{d},\alpha)^{12}\text{C}$ and the $^{14}\text{N}(\text{d},\text{p})^{15}\text{N}$ nuclear reactions whereas the oxygen and carbon ones by the $^{16}\text{O}(\text{d},\text{p})^{17}\text{O}$ and $^{12}\text{C}(\text{d},\text{p})^{13}\text{C}$ (E_d : 1.35 MeV). Investigation of the corrosion behaviour of the samples was performed under strong aggressive conditions (hydrochloric acid 2% at 50 °C) using electrochemical techniques (potentiodynamic polarization and cyclic voltammetry). The samples implanted at 400 °C exhibited remarkable resistance to corrosion compared to those implanted at 500 °C and the untreated material. This could be attributed to the modified surface region and its high nitrogen content.

Keywords: N-implantation; RBS; NRA; corrosion; stainless steel

**Corresponding author: Address: Department of Chemistry, Aristotle University, GR-54124 Thessaloniki, Greece
Tel.: +30 2310 997997, Fax.: +30 2310 997753, E-mail: noli@chem.auth.gr*

1. INTRODUCTION

The high Cr content AISI 304 austenitic stainless steel (Cr 20/Ni 10/Fe) is, due to its excellent corrosion resistance, a material with a wide spectrum of industrial applications. However, it presents poor tribological properties such as hardness and wear resistance. For these reason different techniques have been developed for the

improvement of its surface mechanical properties [1-3]. Nitrogen-ions have widely been used in the past in order to increase the hardness of metallic alloys. However, the austenitic steels are known as materials difficult to be nitrided because the nitridation requires temperatures higher than 450 °C. At these temperatures CrN precipitation takes place leading to a Cr-depleted surface which is susceptible to corrosion and the material loses its stainless character. On the other hand, recently nitridation treatments performed at moderate temperatures (~400 °C) were found to be beneficial for improving the mechanical properties of steels simultaneously enhancing their corrosion resistance. These improvements are associated with the formation of a saturated nitrogen solution (N-content about 20 %) and the nitrogen diffusion into the bulk [4-9]. Of special interest among these nitridation processes is the Low Energy-High Flux Nitrogen-Implantation, which has already been successfully applied to the hardness and corrosion resistance improvement of austenitic stainless steels [5,10-14].

The majority of the publications, which appeared in the literature and concern the influence of the nitridation on the corrosion of stainless steels, are related with studies performed in chlorides solutions (especially NaCl). The published data in these cases show an enhancement of the corrosion resistance of the steels after the N-implantation [15-26].

The aim of this work was to investigate the influence of the nitridation temperature of AISI 304 stainless steel (400 and 500 °C respectively) on its corrosion behavior.

2. EXPERIMENTAL PART

2.1. *Sample preparation*

The AISI 304L stainless steel (Fe, 18.54 Cr, 10.46 Ni, 1.69 Mn, 0.65 Si, 0.016 C) samples used in this work had the form of disks of 1.6 cm diameter and 1.0 mm thickness. Prior to implantation the surface of the samples was mechanically polished using silicon carbide paper (down to 2400 grid) and diamond paste (down to 1.0 μm) leading to a final roughness of about 0.05 μm . Finally, the samples were ultrasonically degreased in acetone and rinsed in 96% ethanol.

The low-energy high-flux nitrogen implantation was performed using a Kaufmann type ion source. The energy of the extracted nitrogen-ions (N^{2+} , N^+) was 1.2 keV and the current density of about 1 mA/cm² providing in 1 hour a total dose of $3,5 \times 10^{19}$ ions/cm². The temperature during the implantation, measured by a thermocouple attached on the back of the samples, was 400 and 500 °C for the two series of implantations performed.

The corrosion resistance of the implanted samples was investigated by potentiodynamic polarization and cyclic voltammetry in 2% HCl at 50 °C using rapid and slow scan measurements. The tests were performed in an AUTOLAB Potentio-Galvanostat (ECO CHEMIE, Netherlands) interfaced to a computer and recorder. The conventional three-electrode cell (EG&G PAR model) used for all measurements, was equipped with a saturated calomel electrode as a reference electrode, a graphite one as an auxiliary electrode and a holder leaving only the one side of the specimen exposed to the corroding medium. Experiments were performed in de-aerated

solution after 5 min stabilisation and scan starting from the open circuit potential in the region -400 up to 1000 mV using the following scan rate; rapid scan rate = 25 mV/sec and slow scan rate = 0.25 mV/sec. In all cases the electrolyte volume was 800 ml and the sample surface in contact with the testing solution 1 cm² [27].

2.2 Characterization of the coatings

The phase composition and the structure of the coatings were investigated by X-Ray Diffraction (XRD), Transmission and Scanning Electron Microscopy (TEM, SEM) whereas their Vickers micro-hardness was also determined [5, 14].

Rutherford Backscattering Spectrometry (RBS) at the 5.5 MV Tandem Accelerator of the NCSR Demokritos/ Athens using deuterons of 1.75 MeV energy (scattering angle: 170°, solid angle: 2.54×10^{-3} sr), was applied in combination with Nuclear Reaction Analysis (NRA) in order to obtain information about the N-, O- and C- depth distribution in the near-surface layers of the samples. The nitrogen depth distribution was determined using the $^{14}\text{N}(\text{d},\alpha)^{12}\text{C}$ and the $^{14}\text{N}(\text{d},\text{p})^{15}\text{N}$ nuclear reactions whereas the oxygen and carbon ones by the $^{16}\text{O}(\text{d},\text{p})^{17}\text{O}$ and $^{12}\text{C}(\text{d},\text{p})^{13}\text{C}$ reactions respectively (E_{d} :1.35 MeV, scattering angle: 150°, solid angle: 0.34×10^{-3} sr). The beam current on the target during the measurements did not exceed 10 nA, while the beam spot size was 1.5×1.5 mm². The analysis of the data was performed by means of the SIMNRA simulation code [28] using cross sections from the IBANDL nuclear data library [29]. The overall uncertainty of the determination was estimated to be ca. 8%.

3. RESULTS AND DISCUSSION

The results of the XRD investigation (not presented here) led to the conclusion that in the case of 400°C N-implantation the incorporation of the nitrogen atoms into interstitial positions resulted in the formation of an nitrogen solid solution in the initial austenitic steel matrix so called “expanded austenite” or γ_{N} phase of fcc crystallographic structure. This induced an expansion of the lattice producing compressive residual stresses and micro-distortions in the N-implanted layer being responsible for the hardness increase. In the 500°C N-implantation CrN and α -FeNi phases were formed because Fe, Cr and Ni atoms were allowed to diffuse. The lattice parameter deduced from the XRD peaks was found to be expanded and the Vickers micro-hardness, compared to that of the non-implanted material, four and five times higher for the two series of samples [5,14].

The oxygen, carbon and nitrogen content in the near-surface layers of the non-implanted and implanted at 400 and 500° samples was measured by NRA. In the case of the sample implanted at 400 °C the oxygen peaks were more intense indicating the formation of a surface oxide layer whereas the nitrogen found to be less diffused. Several authors have reported that the oxygen absorbed during nitrogen implantation is considered to act as barrier to nitrogen transfer into the bulk [7-8, 12, 14]. The carbon concentration for all the samples was found to be between 1.2 and 1.5 % with a maximum depth range of ca. 1.0 μm .

The nitrogen distribution obtained by the SIMNRA simulation of the NRA spectrum (s. Fig. 1) also allows an estimation of the thickness of the modified surface layer (ca.

4 and 6 μm for the samples implanted at 400 and 500 $^{\circ}\text{C}$ respectively). In Fig. 1 the presence of peaks corresponding to particles emitted by the $^{14}\text{N}(\text{d},\alpha_1)^{12}\text{C}$, $^{14}\text{N}(\text{d},\text{p}_0)^{15}\text{N}$ and the $^{14}\text{N}(\text{d},\alpha_0)^{12}\text{C}$ nuclear reactions is obvious.

As demonstrated from the polarization measurements the corrosion resistance of the samples implanted at 400 $^{\circ}\text{C}$ was significantly enhanced. In the case of the samples implanted at 500 $^{\circ}\text{C}$ a slight improvement of the corrosion resistance was observed compared to that of the non-implanted material.

Figure 2 presents the NRA spectra of the samples implanted at 400 and 500 $^{\circ}\text{C}$ after the corrosion attack showing increased oxygen- and carbon concentration in the sample implanted at 500 $^{\circ}\text{C}$. This could be attributed to the higher corrosion rate due to the dissolution and oxidation of the main steel constituents especially Fe and Cr. Concerning the nitrogen distribution no differences were observed compared to the spectra of the non-corroded samples.

The increased corrosion tendency, but lower compared to that of the non-implanted steel, exhibited by the sample implanted at 500 $^{\circ}\text{C}$ can be observed in Fig. 3. The extended corrosion attack in this case is indicated by the missing edge appearing in the region of channels 270 to 330 in the RBS data presented in this figure. No similar effects appeared in the corresponding spectrum of the sample implanted at 400 $^{\circ}\text{C}$ (s. Fig. 4). This means that the implanted samples at 400 $^{\circ}\text{C}$ exhibited a remarkable resistance to the corrosive medium.

The SEM micrographs after the corrosion attack showed a long-standing and uniformly corroded surface of the implanted samples at 400 $^{\circ}\text{C}$ whereas a thick porous corroded zone with large pits was observed on the non-implanted and the sample implanted at 500 $^{\circ}\text{C}$. The Cr-concentration was found to be reduced across this layer (about 10%) demonstrating a Cr-depletion in the surface region due to CrN precipitation taking place during the implantation at high temperatures.

The beneficial effect of N-implantation on the corrosion behaviour of stainless steel could be associated to structural effects (e.g. formation of an amorphous layer) and mainly assigned to chemical reasons as reported in the literature [19-20, 22]. Osozawa and Okata suggested that nitrogen reacts with H^+ -ions in the pits leading to the formation of NH_3 and NH_4^+ . The reaction causes a decrease of the acidity in the pits and the repassivation is thereby enhanced [26]. The results of this work demonstrated an improvement of the corrosion resistance of the N-implanted steel samples associated with the thick nitrogen-containing modified surface region. Even in the case of the implantation at 500 $^{\circ}\text{C}$, despite the CrN precipitation and the Cr-depletion, an improved corrosion resistance, due to the iron nitrides protecting the substrate, was also observed under the testing conditions.

4. Conclusions

The high-dose low-energy nitrogen implantation of AISI 304L steel at 400 $^{\circ}\text{C}$ significantly increases the surface hardness and the corrosion resistance of the material in 2% HCl solution. These effects can be associated with radiation damage and the segregation of nitrogen at the grain boundaries.

The implantation at 500 $^{\circ}\text{C}$ leads to a more drastically increased surface hardness of the AISI 304L steel but the Cr-depletion due to the CrN precipitation taking part at

this temperature influences the corrosion resistance of the material which was found to be low but better than that of the non-implanted steel.

5. Acknowledgements

The assistance of the staff of the Tandem Accelerator Laboratory of the Nuclear Physics Institute of the NCSR Demokritos (Athens/GR) is thankfully acknowledged.

6. References

1. G. Dearneley, Nucl. Instr. and Meth. B 50 (1990) 358.
2. R. Wei, P. J. Wilbur, O. Özturk, D.L. Williamson, Nucl. Instr. and Meth. B 59/60 (1991) 731.
3. L.J. Bredell, J.B. Malherbe, Thin Solid Films 228 (1993) 267.
4. T. Bell, J. Phys. D. 25 (1991) 297.
5. S. Picard, J.B. Memet, R. Sabot, J.L. Grosseau-Poussard, J.P. Rivière, R. Meilland, Mater. Sci. Engin. A303 (2001) 163.
6. C.X. Li, T. Bell Corros. Sc. 48 (2006) 2036.
7. S. Parascandola, O. Kruse, W. Möller, Appl. Phys. Lett. 75 (1999) 1851.
8. C.A. Figueira, F. Alvarez, Surf. Coat. Technol. 200 (2005) 498.
9. T. Christiansen, M.A.J. Somers, Scripta Materialia, 50, (2004) 35.
10. D.L. Williamson, O. Özturk, R. Wei, P.J. Wilbur, Surf. Coat. Technol. 65(1994)15.
11. R. Wei, B. Shogrin, P.J. Wilbur, O. Ozturk, D.L. Williamson, I. Ivanov, E. Metin, J. Tribol. 116 (1994) 870.
12. R. Wei, Surf. Coat. Technol. 83 (1996) 218.
13. G. Abrasonis, J.P. Rivière, C. Templier, A. Declémery, L. Pranevicius, X. Milhet, J. Appl. Phys. 97 (2005), 083531.
14. F. Pedraza, J. L. Grosseau-Poussard, G. Abrasonis, J.P. Rivière, J.F. Dinhut, J. Appl. Phys. 94 12 (2003) 7509.
15. J.P. Hirvonen, D. Ruck, S. Yan, A. Mahiut, P. Torri, J. Likonen, Surf. Coat. Technol. 74-75 (1995) 760.
16. T. Weber, L. de Wit, F.W. Saris, A. Koniger, B. Rauschenbach, G.K. Wolf, S. Krauss, Mater. Sc. Engin. A199 (1995) 205.
17. J. Flis, J. Mankowski, T. Zakkrozymski, T. Bell, S. Janosi, Z. Kolozswary, B. Narowska, Corros. Sc. 41 (1999) 1257.
18. Lei MK., Zhu X.M., Surf. Coat. Technol. 201 15 (2007) 6865.
19. R.F.A. Jargelius-Petterson, Cor. Sci. 41 (1999) 1639.
20. I. Olefjord, L. Wegrelius, Cor. Sci. 38 7(1996) 1203.
21. H-C. Choe, Surf. Coat. Technol. 112 (1999) 299.
22. X. B. Tian, S.C. Kwork, L.P. Wang, P.k. Chu, Mater. Sc. Engin. A326 (2002) 348.
23. V. Muthukumaran, V. Selladurai, S. Nandhakumar, M. Senthilkumar, Mater. Des. 31 (2010) 2813.
24. C.M. Abrieu, M.J. Cristobal, P. Merino, X.R. Novoa, G. Pena, M.C. Perez, Electrochim. Act. 53 (2008) 6000.
25. J.H. Liang, C.S. Wang, W.F. Tsai, C.F. Ai, Surf. Coat. Technol. 1(2007) 6638.
26. K. Osozawa, N. Okato, in: Proc. USA-Japan Seminar:Passivity and its Breakdown on Iron and Iron-Based Alloys, Honolulu, NACE 1976, p.135.

27. Laboratory Corrosion Tests and Standards (Eds. Haynes and Baboian), American Society for Testing and Materials, Philadelphia, 1985.
28. M. Mayer, 'SIMNRA User's Guide 6.0', Max Plank Institut für Plasmaphysik, Garching, Germany, 2006.
29. Ion Beam Analysis Nuclear Data Library, <http://amdu1.iaea.org/ibandl/>.

Figure captions

Fig.1 NRA spectrum presenting the N-distribution of the sample implanted at 400 °C.

Fig.2 NRA spectra of the implanted samples at 400 and 500 °C after the corrosion tests.

Fig.3 RBS-spectra of the implanted samples at 500 °C, before and after the corrosion treatment.

Fig.4 RBS-spectra of the implanted samples at 400 °C, before and after the corrosion treatment.

